

Moxifloxacin Advection: Dispersion in the Blood Stream

Chong Li, Laura Nolt, Paul Scanlon

Colorado State University, Math 435, Spring 2019

Abstract

The purpose of this paper is to explore the dispersion characteristics of drugs in the blood-stream. Specifically, we seek to explore the chances of overdose among allergy prone patients taking the medication AVELOX[®], which contains the substance moxifloxacin. AVELOX[®] is mostly for treating bacterial infections, such as Bronchitis, Pneumonia and prescription level tissue ailments. By exploring advection in a blood circulation sense, we will model injection volume recommendations to lower the risk of a moxifloxacin overdose.

1. Background Information & Introduction

1.1. Pharmacokinetics

Pharmacokinetics is described as the body's action on drugs, which refers to the movement of drugs into, through, and out of the body. It is defined as the study of the time course of drug absorption, distribution, metabolism, and excretion [6]. In other words, it is known as the branch of pharmacology concerned with the movement of drugs within the body [10]. Due to related factors and the chemical characteristics of the drug, most pharmacokinetic studies of a drug depends on the particular patient. Some patient-related factors (e.g, renal function, genetic makeup, sex, age) can be used to predict pharmacokinetic parameters in the population [7]. For example, the half-life of some drugs, especially those requiring metabolism and excretion, may be very long among the elderly. Clinical pharmacokinetics is the application of pharmacokinetic principles to the safe and effective management of medications for individual patients [6]. The main goals of clinical pharmacokinetics include improving efficacy and reducing the toxicity of drug therapy in patients. The development of a strong correlation between drug concentration and its pharmacological response allows clinicians to apply pharmacokinetic principles to actual patient conditions. Understanding the pharmacokinetic principles helps prescribers more accurately and more quickly adjust doses. The application of pharmacokinetic principles to individualized drug therapy is also called therapeutic drug monitoring [6].

2. History/Importance

2.1. History

The term pharmacokinetics was first introduced by F. H. Dost in 1953 in his text, *Der Bliitspiegel-Kinetik der Konzentrationsabläufe in der Frieslauffliissigkeit* (Dost, 1953). The origins of the pharmacokinetic theme are both multinational and multidisciplinary. Investigators in England, Germany, Sweden and the United States have contributed to the

development of pharmacokinetics in different fields. In 1961, a review article entitled "Biopharmaceutics: Absorption Aspects" was published, which attracted the attention of many pharmaceutical and other scientists. This review, along with Nelson's comments (1961), has led to a significant increase in interest in pharmacokinetics. During this period, there were many books on the field of pharmacokinetics. By the end of 1972, several journals had published articles on pharmacokinetics. These examples are: *Journal of Pharmaceutical Sciences*; *European Journal of Clinical Pharmacology* (from Vol. 3, No. 1, December 1970 to date; formerly *Pharmacologia Clinica*); *International Journal of Clinical Pharmacology and Biopharmacy* (formerly *International Journal of Clinical Pharmacology, Therapy and Toxicology*); *Clinical Pharmacology and Therapeutics*; and *Journal of Clinical Pharmacology*. Many who publish in the field of pharmacokinetics want their work to be noticed, so they set up professional journals. Three of the most important are: *Journal of Pharmacokinetics and Biopharmaceutics*, Vol. 1, No. 1, published in February, 1973; *Clinical Pharmacokinetics*, Vol. 1, No. 1, published in January, 1976; and *Biopharmaceutics and Drug Disposition*, Vol. 1, No. 1, published in July-September, 1979. These journals help publishers see each other's articles and communicate with each other, allowing pharmacokinetics to develop and improve rapidly [8]. More books are pictured in Figure 1.

The Mathematical Approach to Physiological Problems (Riggs, 1963)
 Uptake and Distribution of Anesthetic Agents (Papper and Kitz, 1963)
 Pharmacogenetics (Kalow, 1965)
 Drug and Tracer Kinetics (Rescigno and Segré, 1966)
 Grundlagen der Pharmacokinetik (Dost, 1968)
 Multicompartment Models for Biological Systems (Atkins, 1969)
 Biopharmaceutics and Relevant Pharmacokinetics (Wagner, 1971a)
 Biopharmaceutics and Pharmacokinetics: An Introduction (Notari, 1971)
 Guidelines for Biopharmaceutical Studies in Man (Dittert *et al.*, 1972)
 Schering Workshop on Pharmacokinetics (Raspé, 1970)
 Tracer Methods for *In Vivo* Kinetics: Theory and Applications (Shipley and Clark, 1972)

Figure 1: Books Dealing with Pharmacokinetic Principles Published between 1961-1972

2.2. Importance

In the past few years, pharmacokinetics has become an integral part of drug development, especially in determining the biological characteristics of drugs. The pharmacokinetic and metabolic characteristics of drug compounds need to be understood when designing appropriate human clinical trials. Pharmacokinetics makes the drug development process more efficient. To reduce the overall cost of drug development, resources must be focused on the compounds most likely to succeed. The usefulness of pharmacokinetic prediction in the drug discovery phase results in fewer compounds failing. This application of pharmacokinetic prediction is now being extended to the pharmacodynamics of new compounds in order to better understand their efficacy and safety. It is necessary to obtain human pharmacokinetic information for the development of new drugs to ensure the appropriate use of drugs. Conducting clinical pharmacokinetic studies to examine the absorption, distribution, metabolism, and excretion of study or approved drugs in healthy volunteers is vital to drug development. The data obtained from these studies can be used for the design and implementation of follow-up clinical trials. They are also necessary for the proper analysis and evaluation of efficacy and safety data obtained in clinical trials of new drug development and

post-marketing clinical trials. The results of clinical pharmacokinetic studies can be used to determine the appropriate use of drugs based on patient characteristics. [4]

2.3. Improvement

Early termination of failed drug development programs is seen as a way to reduce overall costs. To achieve this, it is important to understand the root causes of wear and tear that have caused drug development failures in the past. A previously published survey of the causes of drug development failure, as shown in Figure 2, indicated that inappropriate pharmacokinetics was a major cause. Inappropriate pharmacokinetic behaviors include factors such as low bioavailability due to high extraction or low absorption characteristics, short elimination half-life due to short action duration, and excessive variability due to genetic or environmental factors. This observation has led to an increasing emphasis on pharmacokinetic inputs throughout the pharmaceutical industry. Most of these issues can be addressed by extending the prediction of pharmacokinetic behavior to include the pharmacodynamic characteristics of candidate drugs. [4]

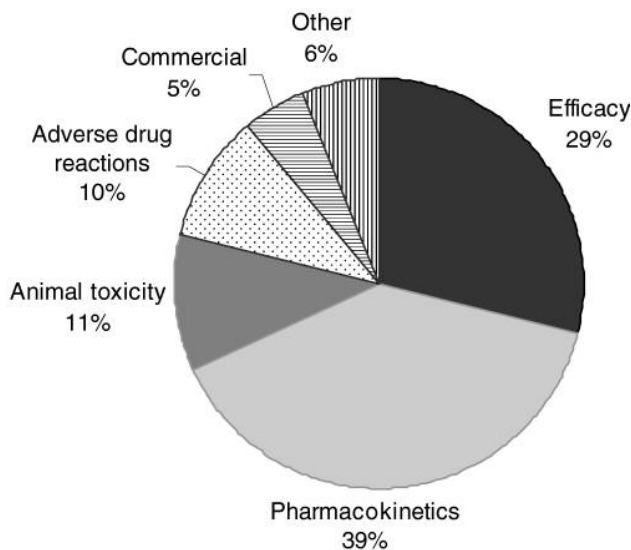


Figure 2: The reasons for failure of drug development programs by the seven UK-based pharmaceutical companies in the period 1964–1985 [4]

3. Moxifloxacin

3.1. About the Medicine

AVELOX[®] produces an injection containing 400mg of moxifloxacin. This medication is used for treatment of varying bacterial infections: Bronchitis, Pneumonia, Sinusitis, complicated skin and skin structure infections, and complicated intra-abdominal infections (including polymicrobial infections such as abscesses). The recommended dosage is 400mg daily; however, duration of treatment depends on severity of the specified bacterial infection. The duration recommendations are as follows: Bronchitis 5 days, Pneumonia 7-14 days, Sinusitis 7 days, complicated skin and skin structure infections 7-21 days, and complicated intra-abdominal infections 5-14 days. AVELOX[®] is administered through either a film-coated

tablet or through a liquid solution injection. Administering the solution requires it be infused intravenously over 60 minutes. [3] For the sake of this report, we will focus on the intravenous nature of the AVELOX[®] medication. Studies of pharmacokinetics among males and females showed that there were differences in body weight and drug effects/absorption. However, this did not lead to any correlations with gender or ethnicity.

3.2. Distribution

The moxifloxacin contained in the AVELOX[®] drug very quickly distributes to extravascular spaces. Extravascular space is "the space that surrounds the cells of a given tissue" [5]. Higher concentration levels of moxifloxacin appear in certain tissues, such as the lungs, sinuses, and abdominal tissues/fluids.

3.3. Warnings & Precautions

This drug is associated with adverse reactions involving the nervous and musculoskeletal systems. For hypersensitivity issues and allergic reactions, these commonly occur after the first dose and can be easily taken care of with immediate contact with a doctor. Very rarely do the allergic reactions lead to anaphylactic shock. However, if this were to occur, the patient would be urged to stop any treatment plans utilizing AVELOX[®] or other drugs containing moxifloxacin. Patients should also be aware of psychiatric reactions that may occur during their treatment. Some of these reactions include, but are not limited to, depression symptoms and psychotic reactions. Therefore, the use of AVELOX[®] is not recommended for patients with a history of psychiatric disease and they need to be cautious of mixing with other medications, such as antidepressants. [3]

3.4. Overdose

Following an injection, peak concentrations of $0.6 - 3.2\text{mg/L}$ of the medicine are detectable in patients at the active site [3]. In our case, the active site is the head/brain of the patient. This is so we can explore the psychological and psychiatric reactions that may ensue due to overdose.

4. Assumptions

In order to create a logical, closed, tubular advection system,

1. We only used data found about moxifloxacin in the AVELOX[®] drug.
2. The 128 node map is an oversimplification of the bloodstream used solely for the sake of this project.
3. Vein size/volume assumptions are very vague for the sake of modeling the drug density.
4. To explore overdose precautions, the active site of our model is when the medication reaches the brain.

5. Blood Flow Mapping

To begin the modeling process, we first needed to create a way to make a path through the bloodstream. Utilizing a representation of the human arterial map, we coded a probabilistic tree model in R. It works to traverse through the 128 different nodes in the arterial map shown in Figure 3. The path through our probabilistic tree model will act in a “circulatory” type of way. Regardless of the injection site, the substance will initially flow in a path away from the heart. We assume this is the case due to the heart continuously pumping blood outwards. As it traverses through the tree, there is equal probability it will take any branch. For example, if there are three different ways the substance can go, there is a $1/3$ chance it will take either of the three branches. Now, the injected medication will eventually hit a stopping point (i.e. a final node at the end of the trees). From here, it will take the shortest path to the heart.

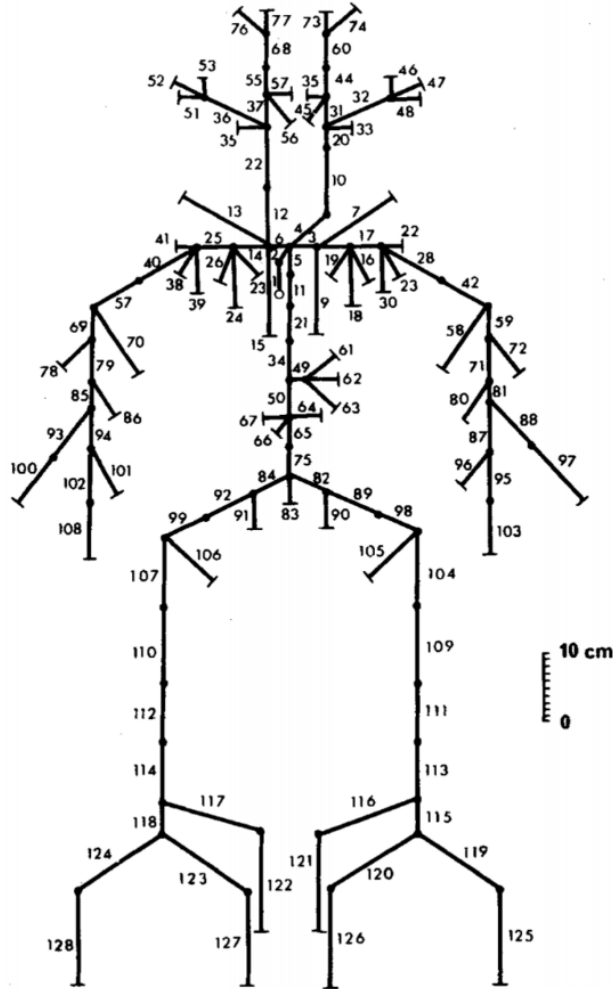


Figure 3: Simplification of the Human Blood Circulation Structure Using the Human Arterial Map [2]

	Left	Right	Length L (cm)	Radius R (cm)	Wall thickness (h cm)	$E \times 10^2$ dyn/cm	f_0 (Hz)
Ascending aorta	1		40	1.45	0.163	4	34.7
Aortic arch	2		2.0	1.12	0.132	4	16.7
Aortic arch	5		3.9	1.07	0.127	4	36.6
Thoracic aorta	11		5.2	1.00	0.120	4	27.6
Thoracic aorta	21		5.2	0.95	0.116	4	27.8
Thoracic aorta	34		5.2	0.95	0.116	4	27.8
Abdominal aorta	50		5.3	0.87	0.108	4	27.5
Abdominal aorta	65		5.3	0.57	0.080	4	29.3
Abdominal aorta	75		5.3	0.57	0.080	4	29.3
Coeliac artery	49		1.0	0.39	0.064	4	167.8
Gastric artery	61		7.1	0.18	0.045	4	29.2
Splenic artery	62		6.3	0.28	0.054	4	28.9
Hepatic artery	63		6.6	0.22	0.049	4	29.6
Renal artery	64		3.2	0.26	0.053	4	58.4
Superior mesenteric	66		5.9	0.43	0.069	4	28.1
Gastric artery	67		3.2	0.26	0.053	4	58.4
Inferior mesenteric	83		5.0	0.16	0.043	4	42.9
Common carotid (L)	4		8.9	0.37	0.063	4	19.2
Common carotid (L)	10		8.9	0.37	0.063	4	19.2
Common carotid (L)	20		3.1	0.37	0.63	4	55.1
Common carotid (R)	12		8.9	0.37	0.063	4	19.2
Common carotid (R)	22		8.9	0.37	0.063	4	19.2
Left subclavian artery	3		3.4	0.42	0.067	4	48.6
Brachiocephalic artery	6		3.4	0.62	0.086	4	45.4
Common iliac		82 84	5.8	0.52	0.076	4	27.3
External iliac		89 92	8.3	0.29	0.055	4	21.3
*Internal iliac		90 91	5.0	0.20	0.040	16	74.1
External iliac		98 99	6.1	0.27	0.053	4	30.1
Femoral artery		104 107	12.7	0.24	0.050	8	21.1
Profundus artery		105 106	12.6	0.23	0.049	16	30.3
Femoral artery		109 110	12.7	0.24	0.050	8	21.1
Popliteal artery		111 112	9.4	0.20	0.047	8	30.2
Popliteal artery		113 114	9.4	0.20	0.050	4	22.0
Anterior tibial artery		115 118	2.5	0.13	0.039	16	181.5
Anterior tibial artery		119 124	15.0	0.10	0.020	16	24.7
Posterior tibial artery		125 128	15.0	0.10	0.020	16	24.7
Posterior tibial artery		116 117	16.1	0.18	0.045	16	25.7
Posterior tibial artery		121 122	16.1	0.18	0.045	16	25.7
*Peroneal artery		120 123	15.9	0.13	0.039	16	28.5
*Peroneal artery		126 127	15.9	0.13	0.019	16	28.5
Carotid (internal)		31 37	5.9	0.18	0.045	8	49.6
External carotid		32 36	11.8	0.15	0.042	8	26.3
*Superior thyroid artery		33 35	4.0	0.07	0.020	8	78.3
*Lingual artery		43 56	3.0	0.10	0.030	8	106.9
Internal carotid		44 55	5.9	0.13	0.039	8	54.4
*Facial artery		45 54	4.0	0.10	0.030	16	113.4
*Middle cerebral		46 53	3.0	0.06	0.020	16	159.4
Cerebral artery		47 52	5.9	0.08	0.026	16	80.0
*Ophthalmic artery		48 51	3.0	0.07	0.020	16	147.6
Internal carotid		60 68	5.9	0.08	0.026	16	80.0
*Superficial temporal		73 77	4.0	0.06	0.020	16	119.6
*Maxillary artery		74 76	5.0	0.07	0.020	16	88.6
*Internal mammary		7 15	15.0	0.10	0.030	8	21.4
Subclavian artery		8 14	6.8	0.40	0.066	4	24.7
Vertebral artery		9 13	14.8	0.19	0.045	8	19.2
*Costo-cervical artery		16 26	5.0	0.10	0.030	8	64.2
Axillary artery		17 25	6.1	0.36	0.062	4	28.2
*Suprascapular		18 24	10.0	0.20	0.052	8	29.9
*Thyro-cervical		19 23	5.0	0.10	0.030	8	64.2
*Thoraco-acromial		27 41	3.0	0.15	0.035	16	133.4
Axillary artery		28 40	5.6	0.31	0.057	4	31.7
*Circumflex scapular		29 39	5.0	0.10	0.030	16	90.7
*Subscapular		30 38	8.0	0.15	0.035	16	50.0
Brachial artery		42 57	6.3	0.28	0.055	4	29.1
*Profunda brachi		58 70	15.0	0.15	0.035	8	18.9
Brachial artery		59 69	6.3	0.26	0.053	4	29.7
Brachial artery		71 79	6.3	0.25	0.052	4	29.9
*Superior ulnar collateral		72 78	5.0	0.07	0.020	16	88.6
*Inferior ulnar collateral		80 86	5.0	0.06	0.020	16	95.6
Brachial artery		81 85	4.6	0.24	0.050	4	41.1
Ulnar artery		87 94	6.7	0.21	0.049	8	42.2
Radial artery		88 93	11.7	0.16	0.043	8	25.9
Ulnar artery		95 102	8.5	0.19	0.462	8	33.9
Interossea artery		96 101	7.9	0.09	0.028	16	58.5
Radial artery		97 100	11.7	0.16	0.043	8	25.9
Ulnar artery		103 108	8.5	0.19	0.046	8	33.9

Figure 4: Centimeter Lengths of Each Artery in the Human Arterial Map [2]

Each artery displayed in the human arterial map can be represented in terms of its length in centimeters; this is displayed in Figure 4. Using these lengths, we can utilize our R code described above to measure the distance of the initial path, plus the length of the shortest path to the heart, plus the length to the brain.

Because of the random nature of paths in our bloodstream, the probabilistic tree model randomly calculates a path from a given node. Therefore, for the differential equations section, we will use a random path given from the R code. This information will give us the total length of our basic circulatory path from an injection site to the heart, then up to the brain.

6. Advection Equation with the Circulatory System

Consider the classic advection equation, also known as the *Linear Transport Equation* with a non-zero initial condition [11]:

$$U_t + cU_x = 0 \quad (1)$$

$$U(0, x) = g(x) \quad (2)$$

$$0 < x < R \quad (3)$$

Advection is the transfer of matter by flow. Specifically for application to the circulatory system, slices of the density of medicine within different segments of the circulatory system are discretized with respect to the map above in Figure 3. Here, U represents the rate of flow of a slice of the density of the medicine in question that is originally injected.

This *hyperbolic partial differential equation* has a *unique solution* when $g(x)$ is reasonably defined on \mathbb{R} . The unique solution can be solved *stepwise* and is represented as:

$$u(x, t) = g(x - ct) \quad (4)$$

To understand more clearly, this is the concentration of detectable medicine compared to the initial condition at the time and distance it will have traveled in a continuously flowing system at an assumed speed. To further enumerate, R is the volume of a closed system, and c is the speed of flow.

Discretization of the time axis is done with an assumption of blood flow speed. Northern Michigan University cites maximum blood flow speed around 40 *cm/sec*. We will assume a single cycle or heart beat is also enough to cover the volume of each closed system. This allows the vertical axis in three dimensions to represent a density slice of the expected original injection site concentration at the time it will have taken to travel here under this speed assumption under the fastest flow conditions.

The slope of the traditional three dimensional advection plot can be thought of as the loss rate between the ends of a closed system. With linear assumptions of the flow differential equation's $g(x)$, a three dimensional density slice visualization offers a snapshot of where statistical losses are lingering and how much of the original injection is closest to the active site in real time. These losses are due to branching to other arteries, veins, and capillaries both visible and not visible on the map, as well as, the convention of fluid flow being smoother in the center of a complex fluid system that includes friction due to density. An example of modeling the results of this equation with a transformation to three dimensions is shown below.

The first three dimensional plot, with many colored rings, shows the general shape of the advection equation in three dimensions where the area between each ring is a volume and consecutive rings on the way down the cone represent consecutive edges on the circulation map. The cone's radial area at each height is a chosen density slice from the initial condition with respect to loss factors followed along the way through the closed system.

Density Visualization for One Measured Edge or Many Consecutive Edges

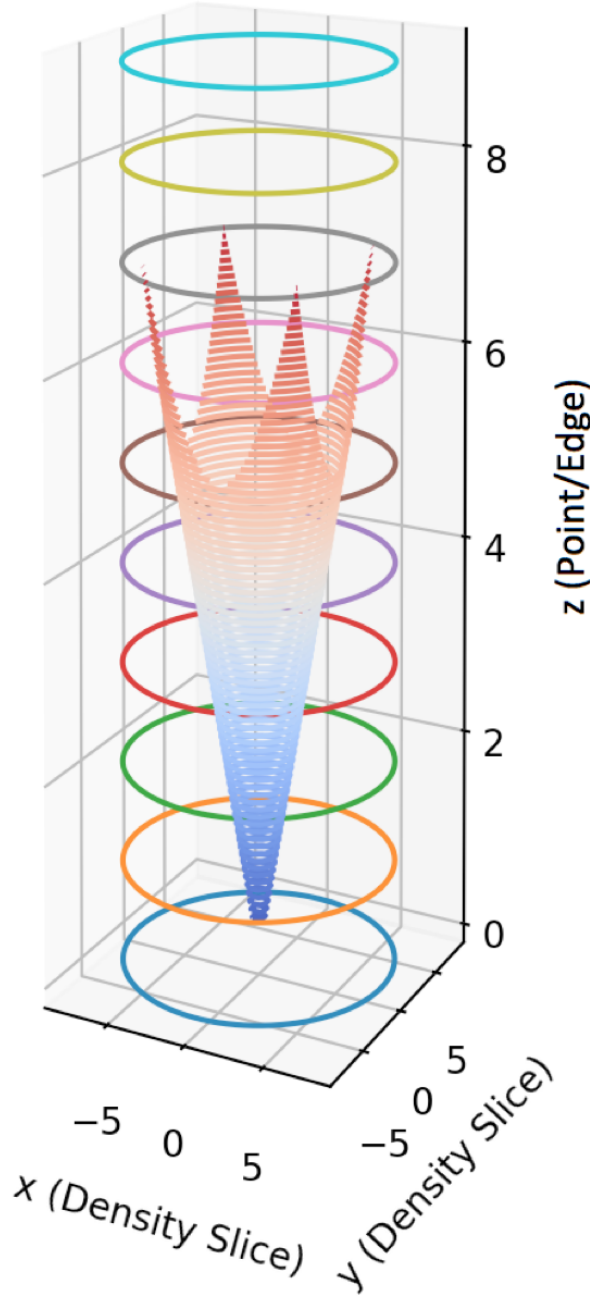


Figure 5: The General Structure of Density Visualization.

The following two plots, with one ring along each of their vertical axes highlighted red instead of blue, model two closed systems that bring the medicine in question, moxifloxacin, to the active site of an allergic individual. The highlighted rings in the latter two three-dimensional plots represents a barrier in the closed system, a heart beat, that produces new systems on each cycle with respect to the major arterial circulation map above.

On the x/y axis, the results of the advection equation for a given system are translated into the shape of a cone. Consideration of a transformation from rectangular to circular coordinates is required. On the z axis, the volume of the system and the edges between, discretized with respect to the map, is depicted. The rate that the cone's radial area diminishes follows the slope of the advection equation's results to the active site, red ring. The cone extends past the red ring to account for loss within a closed system and also discretizing continuous flow over an entire circular path.

7. Modeling Moxifloxacin Advection

For data application to the advection model, the previously described medicine, moxifloxacin, has common psychological and visual side effects in allergic overdose, thus indicating that the active site is in the head. Assuming based on maximum speed of flow and simplification of the circulatory system to major arteries, only two cycles are required to reach the active site. If the density slice can be interpreted as more significant than the data specified overdose density for an allergic individual, a useful recommendation can be made.

For the first closed system, consider the tree between the injection site, heart, and active site. One output from the custom made blood flow statistics algorithm for the tree shows the distance from the injection site to the heart to be 45 *cm* and then 40 *cm* to the active site from the heart; two systems will be enumerated. This fits the distance for approximately one pump per second per system creation by the heart. Slightly low, this is a medically reasonable model.

Along these paths, different radii of circulation will be encountered. Two extremes are the Inferior vena cava artery and the median cubital vein [2]. Their combined average radii is 0.91 *cm*. With a length of 90 *cm* for circulation, the volume is:

$$V = \pi r^2 h \approx 250mL \quad (5)$$

This allows application of moxifloxacin trial data to the advection equation as enumerated by the minimum tested injection volume above. Although the injection is not instantaneous, assuming the worst case for an allergic individual (that the same track of these two systems is followed over the entire injection period) is an extended assumption. The linearity assumption for the density decrease over the volume section yields a form of $g(x)$ such that:

$$g(x) = ax + b \quad (6)$$

Enumerating the variables with this first closed volume section and moxifloxacin clinical trial data yields $a \approx 0.178$, $b \approx 250 \text{ mg}$ and $c \approx 45 \text{ cm/s}$. The a and b values have been optimized for the rough number of branches of smaller radii encountered and flow dynamics. With respect to flow dynamics, it is assumed a significant density is lost due to frictional dispersion dependent on system volume and medicine particle density. Here, for the slope and intercept variables, the application of pharmacokinetics also plays a role. The c approximation is made for the truth value of the system so that the entire volume can be covered in one cycle smoothly. Below is the results of advection in a linear sense.



Figure 6: Flow Equation Optimized to the Heart

Next, the linear model is transformed to three dimensions to fit the previously explained cone. This is achieved by translating the slope into the rate that the cone diminishes between the top edge and edge six, as this is where the heart is encountered in the system [2]. This is a visualization where a partial differential equation's unique solution has been transformed to three dimensional circular coordinate discretization. There are thirteen edges in this chosen system from the custom tree traversal algorithm to model a closed circulation and the heart itself as an additional edge. The heart is considered an additional edge because it infuses blood from additional vena cava arteries [2]. The density with respect to the initial condition in the first system is shown below. The area of the cone at the red ring with its exact density is shown circularly in turquoise, parallel in the z axis (i.e. volume due to flow speed) to this ring as its radial area.

Note : Algorithms implemented for statistical artery mapping, advection, and transformation to three dimensions are included in the *Appendix*.

Density Visualization to the Heart for Moxifloxacin

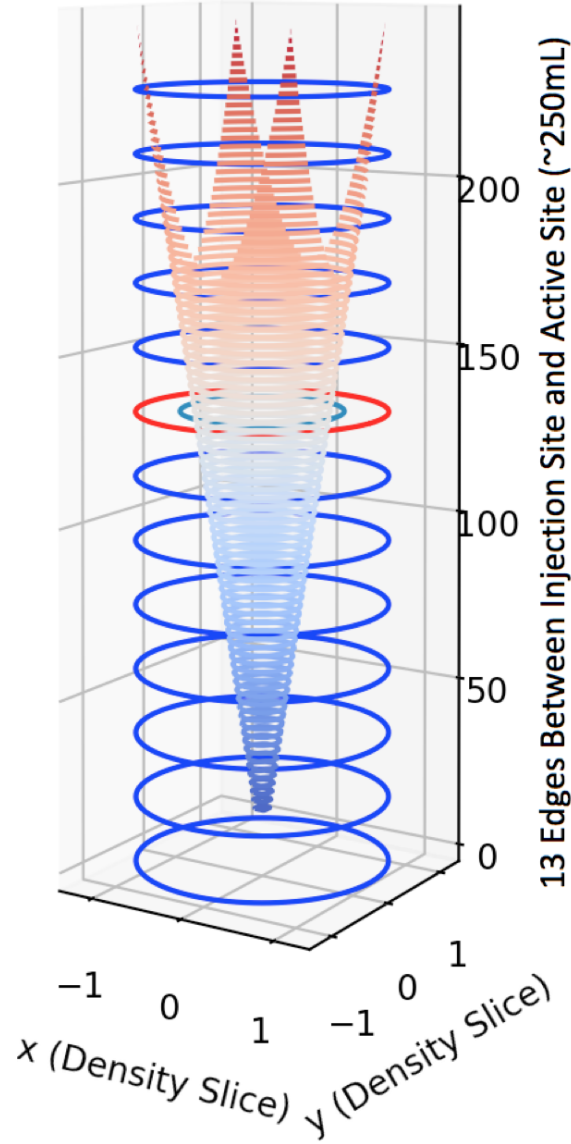


Figure 7: Density of Moxifloxacin Over Closed Circulation to the Heart

From the average speed of circulation in major arteries, a significant density of medicine will have reached the heart in one cycle. This will constitute a new closed system with this density reaching the heart at the speed indicated time. The density at the red ring is observed to be approximately $135 \text{ mg}/250 \text{ mL}$ - indicating a raw 135 mg entering the new system under the new system's volume. The new system will included this density in twice the distance between the active site and the heart, in order to enumerate a new finite circulation system between the heart and the active site [2]. Also the initial value, 135 mg is not 100% of the volume slice as, medically, three times the vena cava should be considered in an additional dispersion time step. This diminishes the concentration of the applicable density slice that has made it to the heart in one cycle by a factor of three.

For the new second system, first consider the volume of the system at the flexible constant enumerated flow speed where there will be 12 edges over an 80 *cm* distance as shown in the tree. The system's volume becomes:

$$V = \pi r^2 h \approx 210mL \quad (7)$$

Enumerating the variables with this second closed volume section and moxifloxacin trial data yields $a \approx 0.268$, $b \approx 210 \text{ mg}$ and $c \approx 40 \text{ cm/s}$.

The same optimization logic with respect to the tree and flow mechanics is applied. Smoothness is considered in the new system between the heart and the active site for vision and psychological ailments. Below is the results of the advection in a linear sense for the second system. Although the initial condition shows density as 100%, this is accounted for by a factor of 1/3 in x and y in the circle production equation for $g(x)$ in three dimensions.

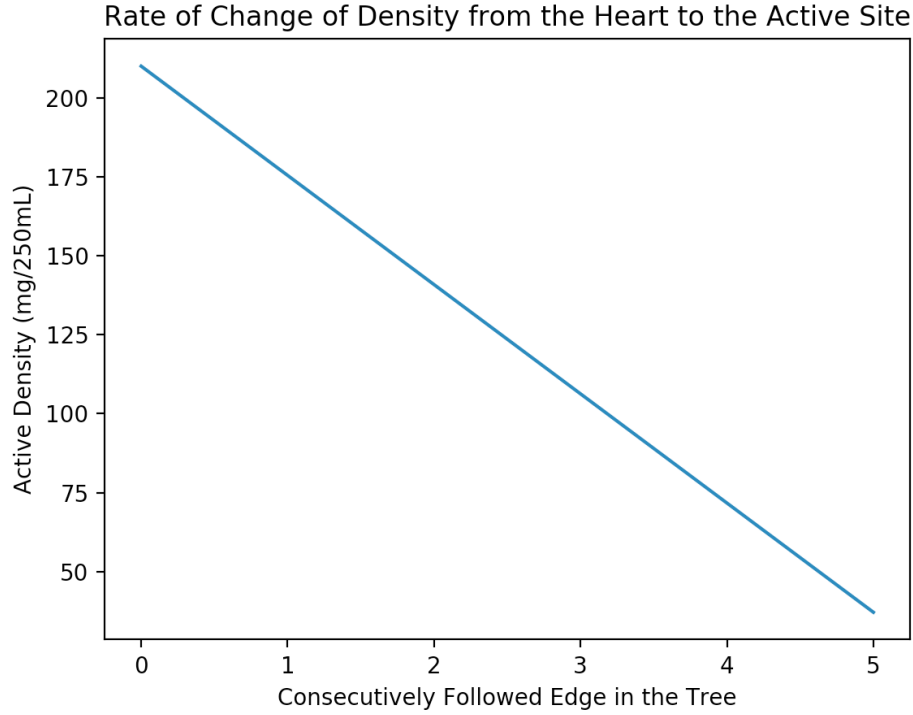


Figure 8: Flow Equation Optimized from the Heart to the Active Site

Next, the linear model is transformed to three dimensions to fit the volume structure of the second system. The cone is not 100% of the volume of the initial ring with respect to global vena cava influx, despite results of the advection equation at the initial time; however, the the advection equation two dimensional plot still represents the decay of the cone to the active site in terms of slope. This is due to the 1/3 factor that is applied. The active site within the brain for psychological/visual ailments in allergic individuals occurs at edge six, which is coincidentally similar to the first system. There are twelve edges here, as the influx of the heart does not matter on this final system to the active site. The density with respect to the initial condition in the first system is shown below by the area of the cone at the red ring, with its exact density shown circularly in turquoise parallel in the z axis to this ring.

Density Visualization from the Heart to the Active Site for Moxifloxacin

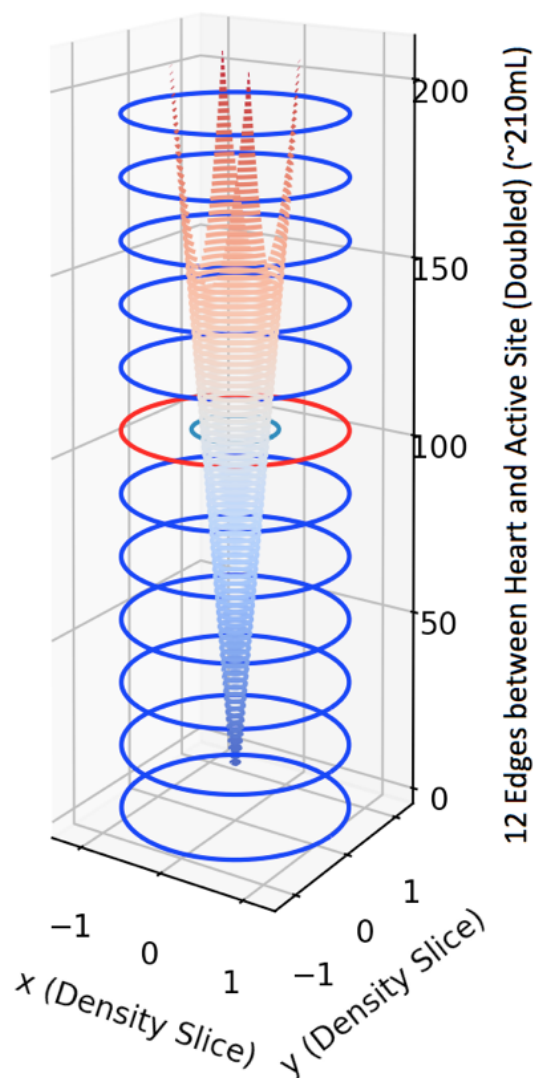


Figure 9: Density of Moxifloxacin Over Closed Circulation from the Heart to the Active Site

A significant density from the heart has now reached the active site. The density at the active site, with respect to all of the previous density loss factors, is approximately 30 $mg/210\text{ mL}$ after accounting for this second system's volume. This is the raw density that interacts with the active site, under the same logic of the previous model interacting with the heart.

This concludes the necessary path along the artery map to make a conclusion about the likelihood of allergic overdose with respect to this medically simplified advection model. AVELOX[®] medical trials' injection volumes do not consider the costs/benefits of including allergic patients with a dosage lower than critical once circulated to the active site. This model shows the extreme over-saturation to an allergic individual.

8. Conclusion

There is 30 *mg* of raw medicine available at the active site from an initial 400 *mg* injection of moxifloxacin. Even assuming just 10% absorption here, an allergic individual is in significant danger of an adverse reaction from the specified pharmacokinetic properties of ailments possible with an absorption of as little as 0.6 *mg* [3].

As cited in the New Zealand Data Sheet, only 0.5% of individuals in the medical trials experienced adverse effects, prompting an allergy warning protocol from AVELOX[®]. However, the medical trials do not have a category for critically sensitive individuals [3]. This drug can be several thousand dollars, when access and availability are considered. The makers and distributors of AVELOX[®] could benefit from considering a safe dosage for allergic individuals. This would improve the outcome of the medical trials with a lower adverse reaction rate and offer increased financial turn around through a larger customer base.

It is recommended from the results of pharmacokinetics, advection modeling, and the simplified arterial map that a trial phase be implemented for anyone taking this drug via injection. As little as 5 *mg* should be the starting volume to stay well out of the adverse reaction range by the end of the dual closed system model for three dimensionally transformed advection. From here, as the days of infusion progress as prescribed, the concentration can be increased to volumes that produce ≥ 0.5 *mg* critical density levels at the active site for an allergic individual, with respect to this model. By gradually introducing the critical concentration (instead of an immediate concentration much higher than critical, as in the clinical trial's data), the comfort and positive effects of moxifloxacin to an allergic patient can be considered. If an allergic patient is able to experience positive effects in the mild critical levels, or even ≤ 0.5 *mg*, the scope of the drug's success will be improved.

9. Distribution of Work

“Nothing fancy. Just team effort, comprised of long hours of good old-fashioned investigative work.” - Raymond King, *The Accountant*, film, 2016.

Bibliography

- [1] Addison Asaa Emily. “Modelling Vehicle Traffic Flow With Partial Differential Equations”. *Jul. 2016*
https://www.researchgate.net/publication/316088790_MODELING_VEHICLE_TRAFFIC_FLOW_WITH_PARTIAL_DIFFERENTIAL_EQUATIONS
- [2] Alberto P. Avolio. “Multi-branched model of the human arterial system” *Medical & Biological Engineering & Computing*
https://www.researchgate.net/profile/Alberto_Avolio/publication/15968016_Multi-branched_model_of_the_human_arterial_system/links/0deec51db2e467bd14000000.pdf
- [3] “AVELOX[®] (Moxifloxacin)”. *New Zealand Data Sheet*
<https://medsafe.govt.nz/Profs/Datasheet/a/AveloxtabIVinf.pdf>
- [4] D K Walker. “The use of pharmacokinetic and pharmacodynamic data in the assessment of drug safety in early drug development”. *British Journal of Pharmacology, 2004*
<https://www.ncbi.nlm.nih.gov/pmc/articles/PMC1884636/>
- [5] “Extravascular space” *Oncology PRO: European Society for Medical Oncology*
<https://oncologypro.esmo.org/Education-Library/Glossary-of-Medical-Terms/extravascular-space>
- [6] “Introduction to Pharmacokinetics and Pharmacodynamics” *Concepts in Clinical Pharmacokinetics*
<https://www.ashp.org/-/media/store%20files/p2418-sample-chapter-1.pdf>
- [7] Jennifer Le. “Overview of Pharmacokinetics”. *Merck Manual, Professional Version*
<https://www.merckmanuals.com/professional/clinical-pharmacology/pharmacokinetics/overview-of-pharmacokinetics>
- [8] John G. Wagner. “History of Pharmacokinetics”. *Pharmacology & Therapeutics, 1981*
<https://deepblue.lib.umich.edu/bitstream/handle/2027.42/24565/0000847.pdf?sequence=1>
- [9] Per Kristen Jakobsen. “An Introduction to Partial Differential Equations”. *11 Jan. 2019*
<https://arxiv.org/pdf/1901.03022.pdf>
- [10] “Pharmacokinetics”. *Wikipedia: The Free Encyclopedia, 2019*
<https://en.wikipedia.org/wiki/Pharmacokinetics>
- [11] “The linear transport equation”. *North Dakota State University*
<https://www.ndsu.edu/pubweb/novozhil/Teaching/483%20Data/02.pdf>

Appendix

R/Python Code

```
}
else if(currentValue == 124) {
  nextValue <- sample(c(seq(1,127),128), 1, prob = c(rep(0,121), 1))
  lengthVec[i] <- 1124
}
else if(currentValue == 125) {
  #nextValue <- sample(c(seq(1,124),125,seq(126,128)), 1, prob = c(rep(0,124), 1, rep(0,3)))
  lengthVec[i] <- 1125
  nextValue <- 0
  shortLength <- 1125+1119+1115+1113+1111+1109+1104+198+189+182+175+165+150+134+121+111+15+12+11
}
else if(currentValue == 126) {
  # nextValue <- sample(c(seq(1,125),126,seq(127,128)), 1, prob = c(rep(0,125), 1, rep(0,2)))
  lengthVec[i] <- 1126
  nextValue <- 0
  shortLength <- 1126+1120+1115+1113+1111+1109+1104+198+189+182+175+165+150+134+121+111+15+12+11
}
else if(currentValue == 127) {
  #nextValue <- sample(c(seq(1,126),127,seq(128,128)), 1, prob = c(rep(0,126), 1, rep(0,1)))
  lengthVec[i] <- 1127
  nextValue <- 0
  shortLength <- 1127+1123+1118+1114+1112+1110+1107+199+192+184+175+165+150+134+121+111+15+12+11
}
else if(currentValue == 128) {
  #nextValue <- sample(c(seq(1,127),128), 1, prob = c(rep(0,121), 1))
  lengthVec[i] <- 1128
  nextValue <- 0
  shortLength <- 1128+1124+1118+1114+1112+1110+1107+199+192+184+175+165+150+134+121+111+15+12+11
}
else{} #if currentValue == 0 we hit a node

xVector[i+1] <- nextValue
currentValue <- nextValue
totalLength <- totalLength + lengthVec[i]
}

#output will be...
#path from our initial point
xVector
#total length (in cm) the tree traversal took until it hit a dead end
totalLength
#total length (in cm) of the shortest path back to the heart
shortLength
```

Figure 10: Snapshot of the Final Lines of R Code Used for the Probabilistic Tree Model (i.e. the human arterial tree)


```

1  import numpy as np
2  import csv
3  import matplotlib.pyplot as plt
4  import scipy.optimize as opt
5  from mpl_toolkits.mplot3d import Axes3D
6  from matplotlib import cm
7
8  def numerical(x, t, g, c): # stepwise
9      est = [0 for i in range(len(x))]
10     for i in range(len(x)):
11         b = x[i]-c*t[i] # unique solution
12         est[i] = g(b)
13     return est
14
15 def g(x):
16     return 210+(0.268*x)
17
18 def circle(x, r): # create circle for visualization
19     o = 0
20     n = (2*np.pi)/x # circular transform coordinants
21     xaxis = [0 for i in range(x)]
22     yaxis = [0 for i in range(x)]
23     for i in range(x):
24         xaxis[i] = r * np.cos(o)
25         yaxis[i] = r * np.sin(o)
26         o = o + n
27     return [xaxis, yaxis]
28
29 def f(x,y): # optomized coefficients 1st system
30     return 204.28* np.sqrt((x) ** 2 + (y) ** 2)
31
32 def f1(x,y): # optomized coefficients 2nd system
33     return 900 * np.sqrt((x/3) ** 2 + (y/3) ** 2)
34
35
36 if __name__ == "__main__":
37     # Arbitrary example, x = 10 cm, t = 10 sec, c = 1/2
38     taxis = range(0,6,1) # time steps
39     taxis = np.array(taxis)
40     xaxis = range(0,6,1) # vein length discritized
41     xaxis = np.array(xaxis)
42     c = 130 # blood flow speed
43     yaxis = [0 for i in range(6)]
44     ex = numerical(xaxis, taxis, g, c)
45     plt.plot(xaxis, ex) # advection
46     plt.xlabel("Consecutively Followed Edge in the Tree")
47     plt.ylabel("Active Density (mg/250mL)")
48     plt.title("Rate of Change of Density from the Heart to the Active Site")
49     plt.show()
50
51     # now lets apply data
52     length = [[] for i in range(10)]
53     for i in range(11):
54         for j in range(1,i+1):
55             length[i-1].append(i)
56
57     fig = plt.figure()
58     ax = fig.add_subplot(111, projection = '3d')
59     r = 4
60     for i in range(10):
61         c = circle(i+1, r)
62         r = r - (1/(i+1))
63         if i != 0:

```

Figure 11: Python Code 1st Half. Used for Advection Modeling.

```

64         ax.scatter(length[i], c[0], c[1], c = 'r', marker = 'o', s = 100)
65         ax.plot(length[i], c[0], c[1])
66     ax.set_xlabel("Location")
67     ax.set_ylabel("x axis")
68     ax.set_zlabel("y axis")
69     plt.show() # general 3d form
70
71     test = circle(100, 1.202082)
72     rings = [[0 for i in range(100)] for j in range(13)]
73     for i in range(13):
74         for j in range(100):
75             rings[i][j] = i*18.9
76     x = np.linspace(-0.85, 0.85, 20)
77     y = np.linspace(-0.85, 0.85, 20)
78     X, Y = np.meshgrid(x, y)
79     R = f(X, Y)
80     fig = plt.figure()
81     ax = plt.axes(projection='3d')
82     ax.set_aspect(3)
83     ax.contour3D(X, Y, R, 100, cmap=cm.coolwarm)
84     ax.set_xlabel('x (Density Slice)')
85     ax.set_ylabel('y (Density Slice)')
86     #ax.set_zlabel('z (Point/Edge)')
87     blood = circle(100, 0.78)
88     ax.plot(blood[0], blood[1], rings[7])
89     for i in range(13):
90         if i == 7:
91             ax.plot(test[0], test[1], rings[i], c = 'r')
92         else:
93             ax.plot(test[0], test[1], rings[i], c = 'b')
94     ax.set_title("Density Visualization for One Measured Edge or Many Consecutive Edges")
95     plt.show()
96
97     test = circle(100, 1.202082) # circular transform
98     rings = [[0 for i in range(100)] for j in range(12)]
99     for i in range(12):
100         for j in range(100):
101             rings[i][j] = i*17.5 # circular transform
102     x = np.linspace(-0.49, 0.49, 20)
103     y = np.linspace(-0.49, 0.49, 20)
104     X, Y = np.meshgrid(x, y)
105     R = f1(X, Y)
106     fig = plt.figure()
107     ax = plt.axes(projection='3d')
108     ax.set_aspect(3)
109     ax.contour3D(X, Y, R, 100, cmap=cm.coolwarm)
110     ax.set_xlabel('x (Density Slice)')
111     ax.set_ylabel('y (Density Slice)')
112     #ax.set_zlabel('z (Point/Edge)')
113     blood = circle(100, 0.46)
114     ax.plot(blood[0], blood[1], rings[6])
115     for i in range(12):
116         if i == 6:
117             ax.plot(test[0], test[1], rings[i], c = 'r')
118         else:
119             ax.plot(test[0], test[1], rings[i], c = 'b')
120     ax.set_title("Density Visualization for One Measured Edge or Many Consecutive Edges")
121     plt.show()

```

Figure 12: Python Code 2nd Half. Used for Advection Modeling.